Acta Cryst. (1996). B52, 1036–1047

Hexamethylenetetramine Suberate, a Strongly Anharmonic Modulated Structure

VALÉRIE BUSSIEN GAILLARD, WŁODZIMIERZ PACIOREK, KURT SCHENK AND GERVAIS CHAPUIS*

Université de Lausanne, Institut de Cristallographie, BSP Dorigny, CH-1015 Lausanne, Switzerland. E-mail: gervais.chapuis@ic.unil.ch

(*Received 20 June 1995; accepted 24 July 1996*)

Abstract

Hexamethylenetetramine suberate is an organic compound presenting a one-dimensional modulation with strong satellite reflections between 123 and 300 K. Single-crystal X-ray intensities of main reflections and satellites up to fourth order have been measured and used for refining a model based on displacive atomic modulation functions. Harmonic terms up to eighth order were necessary to describe the strongly anharmonic modulation. The structure consists of alternating sheets of hexamethylenetetramine and suberic acid connected by hydrogen bonds. Each layer of suberic acid chains consists of alternating areas, each of which is characterized by a common orientation for all chains. These orientations subtend an angle of roughly 60°. At the interfaces, neighbouring chains in adjacent areas adopt intermediate orientations. The two carboxyl groups participate in hydrogen bonds, the character of which depends on the internal coordinate t. In one group and for all values of t, the same oxygen forms a double bond with the α-carbon and the other a single bond, and in the other the carboxylate form is observed for all values of t. The packings of both moieties are incompatible and are conjectured to be responsible for the incommensurability of the structure.

1. Introduction

In the last two decades the study of incommensurate structures has grown exponentially. In Cummins' (1990) and van Smaalen's (1995) compilations mainly inorganic and organometallic compounds have been reported. Most present harmonic modulations with a modulation vector varying with temperature. Frequently, the structures could be described by periodic harmonic distortions of a basic structure derived from the main reflections (de Wolff, Janssen & Janner, 1981). In the rare cases of purely organic compounds, however, only first- or rarely second-order satellites have been included in a full structure refinement.

Among the manifold of incommensurate crystals, hexamethylenetetramine (or hexamine) suberate occupies a particular position. This organic structure contains nothing but light atoms (N, C, O, H) yet displays satellites up to fourth order. In this report the incommensurate structure of hexamine suberate is described on the basis of single-crystal X-ray diffraction data at room temperature.

2. Experimental

The adduct of $N_4(CH_2)_6.(CH_2)_6(COOH)_2$ has been formed by mixing stoichiometric amounts of hexamine and suberic acid in ethanol for 1 h at 350 K. Single crystals were grown by recrystallization in acetonitrile. For the measurements their faces were protected from the humidity of the ambient atmosphere by a film of silicone oil (Paratone). The density of the crystal was measured by floatation in benzene–carbon tetrachloride.

Precession photographs, taken at room temperature, revealed monoclinic symmetry (Fig. 1) with a one-dimensional planar modulation vector. The following reflection conditions were observed: $0k00$, $k = 2n$, and $h0lm$, $m = 2n$, with the monoclinic axis **b**. These conditions indicate the superspace group $P2_1/m(\alpha 0\gamma)0s$ (number 11.2 in *International Tables for Crystallography*, 1993, Vol. C, pp. 800–826). The non-standard setting was chosen in analogy to periodic structures of similar aliphatic diacids (*e.g.* Housty & Hospital, 1965; Gao, Weber & Craven, 1994). No diffuse scattering appeared on the precession photographs.

A DSC analysis of the compound revealed a single phase transition of second order at 363 K. This result is confirmed by precession photographs at different temperatures. The components of the modulation vector are almost invariant between 300 and 123 K.

A single crystal was measured at room temperature on a Syntex $P2_1$ diffractometer (driven by a modified version of $P3$ for satellite measurements) with Cu $K\alpha$ radiation (2θ–ω scans, graphite monochromator). 20 centred main reflections ($21 \le 2\theta \le 76°$) were used to evaluate the cell parameters. The components of the modulation vector $\mathbf{q} = \alpha\mathbf{a}^* + \gamma\mathbf{c}^*$ were obtained by averaging the fractional parts of $\mathbf{a}^*$ and $\mathbf{c}^*$ over 16 centred satellites of the order 1–4 ($15 \le 2\theta \le 37°$). The full width at half-maximum (FWHM) values are remarkably similar for main and satellites reflections in the same range of intensities (Table 1).

Main and satellite reflections were chosen for standards. Both categories of reflections presented identical linear decays of $\sim$20% during some 900 h of

measurement. The reflections of half a sphere were collected; 13 very strong reflections had to be remeasured at different voltage settings of the X-ray tube, thus requiring a second scale factor. No violation of the reflection conditions given above was detected. The data reduction included scaling based on the six standard reflections, an absorption correction based on the crystal shape and orientation, a Lorentz–polarization correction and averaging of equivalent reflections in accordance with the superspace-group symmetry. The resulting data set included 4980 unique reflections. Table 1 summarizes the measurement conditions and Table 2 lists the representative elements of the superspace groups $P2_1/m(\alpha 0\gamma)0s$ and $P2_1(\alpha 0\gamma)$.

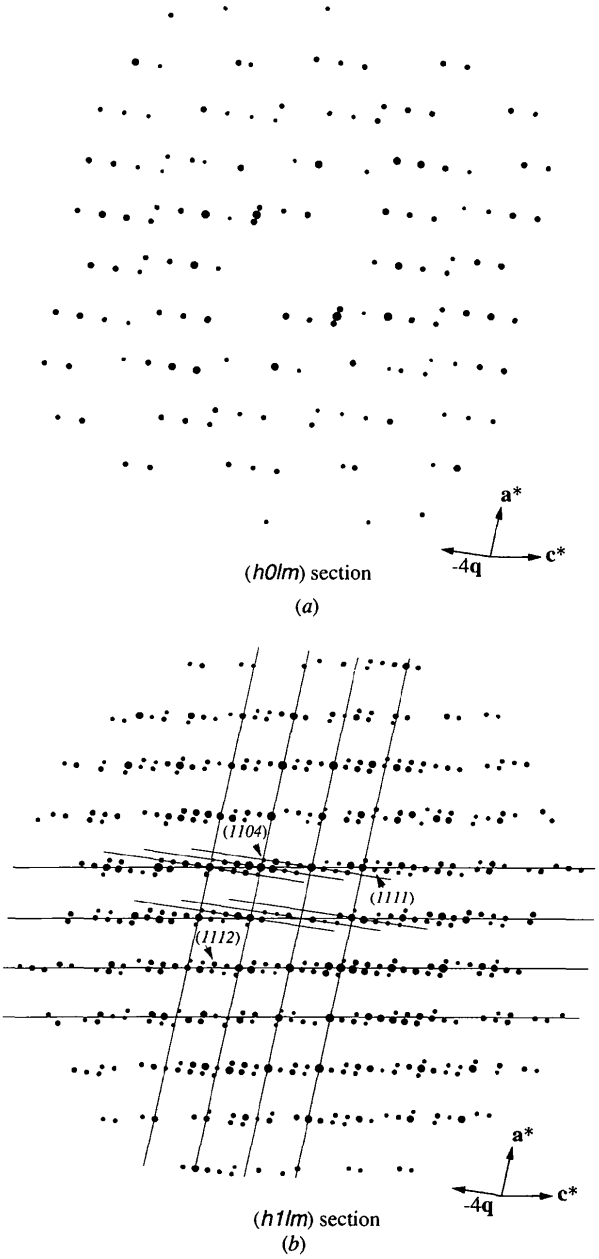

Fig. 1. (*a*) and (*b*) schematic representations of two layers of the reciprocal space. The size of the dots is proportional to the intensities of the peaks. Only reflections larger than 3σ are represented.

3. Structure determination and refinement

3.1. *Structure determination of a commensurate approximation*

From the main reflections only, no basic structure could be determined, neither from direct nor any other methods (*e.g.* Patterson map). Adding the intensities of the satellites to the intensities of their respective main reflections and using these modified reflections for the structure solution also failed. In order to obtain a relevant starting model for the incommensurate refinement a commensurate approximation was made.

Since $\alpha \simeq 0$ and $\gamma \simeq \frac{1}{4}$ the following supercell was chosen

$$\mathbf{a}^{*\prime} = \mathbf{a}^*, \mathbf{b}^{*\prime} = \mathbf{b}^* \text{ and } \mathbf{c}^{*\prime} = \frac{1}{4}\mathbf{c}^*. \quad (1)$$

The indices in the cell (1) become

$$h' = h, k' = k, l' = 4l \text{ for main reflections;}$$
$$h' = h, k' = k, l' = 4l + m \text{ for satellite reflections.} \quad (2)$$

The transformation (2) leads to the following reflection conditions: $h'0l'$, $l' = 2n$, and $0k'0$, $k' = 2n$, corresponding to space group $P2_1/c$. Note that this space group is an artefact due to the transformation of the original cell. It was, however, used for the structure determination.

With the approximations (1) and (2) the structure could be solved by direct methods using the *XS* program of the *SHELXTL* package (Sheldrick, 1978). Two independent hexamines and two independent acid chains could be located on an *E* map. The zigzag planes of the acid chains subtend an angle close to 60° (Fig. 2). The model was refined using *SHELXL*93 (Sheldrick, 1993). For this refinement, only a limited set of data has been used, namely only those values with $|m| = 0$ and 1. In addition to $P2_1/c$, the non-centrosymmetric space group $P2_1$ was also tested. Below are the respective results.

	No. of reflections	No. of parameters	*wR*
$P2_1/c$	2385	399	0.0982
$P2_1$	2385	795	0.0688

The anisotropic displacement parameters (ADP's) were refined for all non-H atoms in both models. The hydrogen positions were deduced from the geometry of the CH_2 groups; bond lengths were restricted to literature values (Housty & Hospital, 1965; Becka & Cruickshank, 1963). Planar restraints were used for the chains of suberic acid.

Table 1. *Summary of crystal and experimental data*

Morphology	{001}, {010}, {1$\bar{1}\bar{1}$}, {110}, {$\bar{2}$10}
Crystal habit	Tabular (platelet)
Dimensions (mm)	0.05 × 0.3 × 0.3
Superspace group	$P2_1(\alpha 0\gamma)000$
Lattice parameters (Å, °, 295 K)	$a = 5.9078(5)$, $b = 24.5423(22)$, $c = 5.9151(6)$
	$\beta = 102.039(7)$
Lattice parameters (Å, °, 123 K)	$a = 5.835(1)$, $b = 24.202(2)$, $c = 5.813(1)$
	$\beta = 101.59(1)$
Volume (Å^3, 295 K)	838.77(13)
Volume (Å^3, 123 K)	804.2(3)
Modulation vector (295 K)	$\mathbf{q} = -0.035(5)\mathbf{a}^* + 0.241(5)\mathbf{c}^*$
Modulation vector (123 K)	$\mathbf{q} = -0.035\mathbf{a}^* + 0.242\mathbf{c}^*$
Z	2
M_r (g mol^{-1})	314.39
D_m (g cm^{-3})	1.26
D_x (g cm^{-3})	1.24
λ (Å)	1.5418
μ (mm^{-1})	0.76
$F(000)$	340
T (K)	295 (2)
2θ range (°)	$3 \le 2\theta \le 115$
$hklm$ range	$-7 \le h \le 7, 0 \le k \le 26, -7 \le l \le 7, -4 \le m \le 4$
$hklm_{max}$	7,26,7,3 ($-3 \le m \le 3$), 4,15,4,4 ($-4 \le m \le 4$)
$(\sin\theta/\lambda)_{max}$ (Å^{-1})	0.592 ($-3 \le m \le 3$), 0.531 ($-4 \le m \le 4$)
Scan width (°)	0.90 (above $K_{\alpha 1}$, below $K_{\alpha 2}$)
Scan speed (° min^{-1})	1.04–14.65
Standard main reflections	11$\bar{1}$0, 2,10,1,0, 13$\bar{2}$0, 6200
Standard satellite reflections	$\bar{1}$30$\bar{1}$, $\bar{1}$$\bar{1}$03
FWHM ($hklm$, °, value)†	1301, 0.12, 1330; 4$\bar{1}\bar{1}$0, 0.20, 797; $\bar{1}$004, 0.17, 250

	All	$m = 0$	$m = \pm 1$	$m = \pm 2$	$m = \pm 3$	$m = \pm 4$
Number of measured reflections	17548	2232	4502	4492	4547	1775
Number of reflections [$I \ge 3\sigma(I)$]	9073	1516	2938	2589	1512	518
Independent reflections [$I \ge 3\sigma(I)$]	4980	821	1564	1429	858	308
Average intensities† [$I \ge 3\sigma(I)$]		19794	9137	2146	926	712
R_{int} without absorption correction	0.024	0.02	0.025	0.035	0.044	0.056
R_{int} with absorption correction	0.022	0.018	0.022	0.032	0.042	0.055

Weights	$w = 1/\sigma^2(F)$
Absorption factor	1.150–1.3930

† Average as a function of $|m|$ over the measured reflections with $I > 3\sigma(I)$.

3.2. *Refinement of the incommensurate structure*

3.2.1. *Theoretical remarks.* The incommensurate structure was refined with a modified version of the *MSR* program (*Modulated Structure Refinement*; Paciorek, 1991). Two possible parametrizations of the atomic modulation functions (MF's) are implemented in this program

$$u_i^\mu(\bar{x}_4^\mu) = \sum_{n>0} [c_{i,n}^\mu \cos(2\pi n\bar{x}_4^\mu) + s_{i,n}^\mu \sin(2\pi n\bar{x}_4^\mu)] \quad (3)$$

or

$$u_i^\mu(\bar{x}_4^\mu) = \sum_{n>0} a_{i,n}^\mu \sin[2\pi(n\bar{x}_4^\mu + \varphi_{i,n}^\mu)]. \quad (4)$$

Both expressions are equivalent, but (3) was preferred because of its superior numerical stability. The significance of the fourth coordinate varies with different authors (Paciorek, Bussien Gaillard, Schenk & Chapuis, 1996). The most common choice used for this parameter is

$$\bar{x}_4^\mu = \mathbf{q}.\mathbf{r}_n^\mu + t, \quad (5)$$

Table 2. *Representative elements of the superspace groups (a) $P2_1/m(\alpha 0\gamma)0s$ and (b) $P2_1(\alpha 0\gamma)$, with monoclinic axis **b** and origin on 1*

(a)	1	$\{x, y, z, t\}$	(b)	1	$\{x, y, z, t\}$
	2_1	$\{-x, y+\frac{1}{2}, -z, -t+\frac{1}{2}\}$		2_1	$\{-x, y+\frac{1}{2}, -z, -t\}$
	m_y	$\{x, -y+\frac{1}{2}, z, t+\frac{1}{2}\}$			
	$\bar{1}$	$\{-x, -y, -z, -t\}$			

where $\mathbf{r}_n^\mu$ specifies the basic coordinate $\mathbf{r}_0^\mu$ of the μth atom in the nth unit cell and t is a continuous function between 0 and 1 representing the mapping of all the basic cells of the crystal onto the original one. Other expressions have been used for the internal coordinate $\bar{x}_4^\mu$, in particular by Kobayashi (1974)

$$\bar{x}_4^\mu = \mathbf{q}.\mathbf{n}^\mu + t, \quad (6)$$

where $\mathbf{n}^\mu$ indicates the nth unit cell where the μth atom is located. Form (6) is especially convenient if constraints have to be applied to the MF's. Expression (6) represents an origin shift of the MF's with respect to (5). The

influence of the choice of the reference point of the MF's on the structure-factor expression is described by Paciorek, Bussien Gaillard, Schenk & Chapuis (1996). Our results presented below have been obtained with Kobayashi's choice of the internal coordinate.

Particular attention has been paid to the inclusion of H atoms in the structure in order to avoid supplementary MF's. The coordinates of an atom riding on a refined one can be directly deduced for each value of the internal coordinate (Paciorek, Bussien Gaillard, Schenk & Chapuis, 1996).

The behaviour of our structure refinements made it plainly clear that restraints were necessary for maintaining a chemically plausible structure. For this purpose various geometrical restraints have been implemented in MSR and used in the results presented in this paper.

3.2.2. *Refinement of the incommensurate model.* In order to initiate the refinement of the incommensurate structure, two hexamines and two acid chains (1 and 4 in Fig. 2) were projected onto the original cell and their coordinates averaged to obtain one unit of hexamine suberate. The two H atoms of the COOH groups, namely H2 and H31 (Fig. 3), could not be located on a difference-Fourier map. Consequently, their positions were calculated from the positions of the COO atoms (Gao, Weber & Craven, 1994). All atoms are located on general positions and, accordingly, no symmetry restrictions were applied. The atomic coordinates and MF's were refined in $P2_1(\alpha 0\gamma)$ (see the justification in §4.2). In the refinement H2 and H31 were also considered as modulated. ADP's were refined for all non-H atoms and isotropic displacement parameters were refined for H2 and H31. The H atoms of the CH_2 groups, representing more than 16% of the electron density of the compound, were included in the refinement as riding atoms (see §3.2.1). Individual isotropic displacement parameters have been refined for these hydrogens.

All classes of reflections were refined simultaneously. An isotropic extinction correction was applied

$$F_{\rm calc}^{\rm corr} = F_{\rm calc}/(1 + 10^{-5} C_{\rm ext} F_{\rm calc}^2/\sin\theta)^{1/4}, \qquad (7)$$

where $C_{\rm ext}$ was refined by MSR. The Axe correction (Axe, 1980) applied in this refinement

$$F_c^{\rm corr} = F_c \exp[-|m|(|m|-1)C_{\rm axe}] \qquad (8)$$

had a particularly significant influence on higher-order satellites. This correction, based on a global phase fluctuation, rescaled properly the partial overall scaling ratios $(\mathrm{OSR})_m$

$$\mathrm{OSR}_m = \Sigma F_{\rm c,m}/\Sigma F_{\rm o,m} \qquad (9)$$

which were systematically overestimated for the satellites (Table 3).

It is interesting to note that the first-order terms of the MF's were not sufficient to reproduce the satellite intensities, especially those of third and fourth order. Additional harmonic terms up to fourth order (the highest order of measured satellites being four) were included, but the high-order satellite intensities were still not satisfactorily reproduced. In order to improve the model, harmonics up to the eighth order had to be included, which decreased drastically the agreement factor for satellites of third and fourth order (Table 3).

The atomic coordinates and ADP's of the structure at $t = 0.0$ are presented in Tables 4 and 5.* The errors were calculated according to Rollet (1965).

Restraints on intramolecular distances and angles were strongly weighted in the refinements to avoid unreasonable geometries of the molecules, particularly of the acid chain. The main effect was to keep the average geometry within expected values and to prevent too large variations of the extrema as a function of t (Table 6). The restraints of the terminal groups were slightly released towards the end of the refinement in order to detect conformational changes of the acid or carboxylate form of COOH as a function of t. Standard deviations have been calculated according to Paciorek, Madariaga & Zúñiga (1991).

For each value of t, a difference-Fourier map was calculated to detect the largest residual densities. No peaks

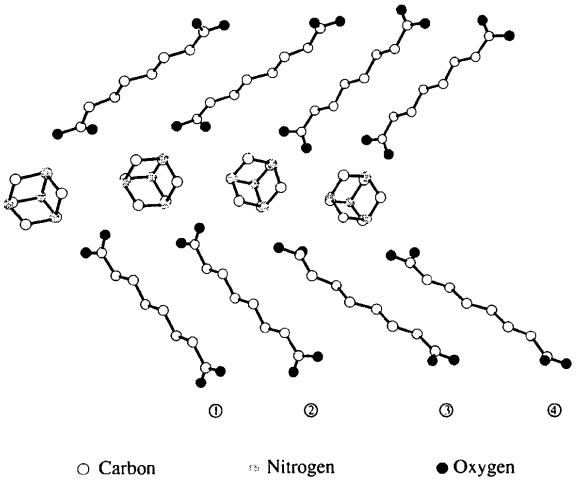

Fig. 2. Projection along **c** of a commensurate approximation of hexamine suberate solved by direct methods in space group $P2_1/c$.

* Lists of atomic coordinates, modulation amplitudes, complete geometry and structure factors have been deposited with the IUCr (Reference: JS0028). Copies may be obtained through The Managing Editor, International Union of Crystallography, 5 Abbey Square, Chester CH1 2HU, England.

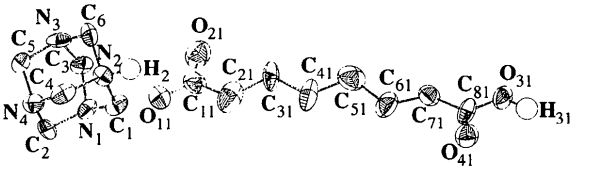

Fig. 3. Representation of hexamine suberate at $t = 0.0$. The ADP's are represented at the 50% probability level (*ORTEP*; Johnson, 1965).

Table 3. *R factors for the modulated structure, with Axe correction*

	Four harmonics			Eight harmonics			Eight harmonics (without Axe correction)		
Number of reflections*	4969			4969			4969		
Number of parameters	431			1364			1363		
m	*R*	*wR*	OSR_m	*R*	*wR*	OSR_m	*R*	*wR*	OSR_m
−4	0.315	0.340	0.8998	0.180	0.175	0.9646	0.356	0.365	1.280
−3	0.225	0.231	0.9529	0.138	0.132	0.9812	0.200	0.185	1.100
−2	0.156	0.156	1.0068	0.086	0.088	1.0039	0.110	0.107	1.007
−1	0.105	0.126	0.9949	0.066	0.079	1.0028	0.103	0.092	0.965
0	0.099	0.067	0.9679	0.068	0.053	0.9802	0.062	0.087	0.956
1	0.103	0.122	0.9973	0.065	0.075	1.0078	0.100	0.092	0.972
2	0.143	0.153	0.9933	0.082	0.082	0.9984	0.098	0.094	1.001
3	0.226	0.223	0.9589	0.130	0.117	0.9806	0.190	0.200	1.110
4	0.306	0.331	0.9574	0.175	0.173	1.0243	0.420	0.435	1.380
All satellites	0.141	0.156	0.9898	0.084	0.089	1.0005	0.130	0.120	1.010
All reflections	0.130	0.112	0.9839	0.079	0.070	0.9950	0.096	0.110	0.995
Goodness-of-fit		5.5744			3.7669			5.2475	
Number of restraints		99			99			99	
Axe correction		0.0614 (14)			0.0529 (16)			—	
Extinction correction		7.18 (47)			8.28 (42)			8.23 (42)	

* The observation condition for a reflection is $I > 3\sigma(I)$ in MSR. For this reason the number of reflections observed in Table 1 is 4980 and 4969 reflections are used by MSR.

Table 4. *Fractional atomic coordinates at t = 0*

	x	*y*	*z*
N1	1.1243 (4)	0.2583 (9)	0.4710 (4)
N2	0.7782 (8)	0.2023 (9)	0.4285 (8)
N3	0.8499 (4)	0.2752 (9)	0.7105 (4)
N4	0.7521 (8)	0.3000 (9)	0.3170 (8)
C1	1.0280 (9)	0.2028 (9)	0.4298 (11)
C2	0.9921 (8)	0.2924 (9)	0.2843 (12)
C3	1.0955 (5)	0.2782 (9)	0.6990 (5)
C4	0.6509 (5)	0.2459 (9)	0.2778 (5)
C5	0.7400 (16)	0.3187 (9)	0.5525 (8)
C6	0.7743 (11)	0.2168 (9)	0.6715 (9)
O11	0.4594 (10)	0.1277 (9)	0.3329 (11)
O21	0.6204 (10)	0.1205 (9)	0.0264 (11)
O31	−0.4405 (10)	−0.0953 (9)	−1.2068 (11)
O41	−0.5808 (12)	−0.0988 (9)	−0.8959 (10)
C11	0.4607 (11)	0.1105 (9)	0.1274 (13)
C21	0.2681 (14)	0.0718 (9)	0.0372 (14)
C31	0.2744 (12)	0.0451 (9)	−0.1894 (13)
C41	0.0620 (13)	0.0128 (9)	−0.2915 (12)
C51	0.0358 (14)	−0.0144 (9)	−0.5217 (15)
C61	−0.2017 (12)	−0.0373 (9)	−0.6233 (12)
C71	−0.2425 (12)	−0.0478 (9)	−0.8799 (13)
C81	−0.4479 (11)	−0.0816 (9)	−0.9856 (11)
H2	0.7370 (73)	0.1638 (19)	0.3809 (19)
H31	−0.5913 (77)	−0.1090 (16)	−1.2877 (82)

or holes indicating missing or misplaced atoms were detected. The most important residua were observed close to the ends of the chains around the COOH groups. The results are presented in Fig. 4 for up to fourth order and up to eighth-order harmonic MF's. The residual electron density is smaller with additional harmonics.

In order to reveal systematic errors in the measurements, particularly for higher-order satellites, different statistical tests were performed on each class of reflections. The normal probability plots (*International Tables for X-ray Crystallography*, 1974, Vol. IV, pp. 293–294) presented in Fig. 5 justify the assumption of normal error distribution, except for a small number of points at the extremities. No abnormal behaviour could be detected from the statistics.

4. Results and discussion

4.1. *The incommensurate structure*

4.1.1. *General features of hexamine suberate.* This structure is characterized by a sequence of alternating sheets of hexamine and suberic acid linked by hydrogen bonds. The zigzag planes of the acid chains are roughly parallel to one of the mirror planes of the hexamine (point-group symmetry $\bar{4}3m$).

The projections of the structure along the **a**, **b** and **c** axes (Fig. 6) reveal a herringbone arrangement of chains separated by sheets of hexamines. A similar disposition of the aliphatic chains has previously been observed

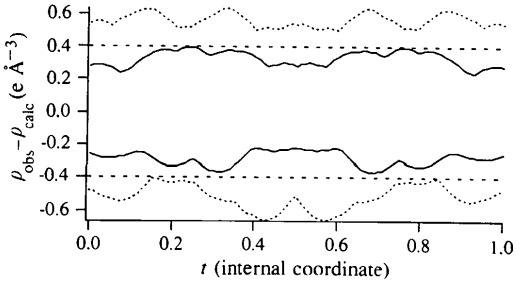

Fig. 4. Minimal and maximal residual electronic density calculated for 100 values of t between 0.0 and 1.0. These values do not exceed ±0.4 e Å^{-3} for eighth-order harmonics and 0.6 e Å^{-3} for fourth-order harmonics.

Table 5. *Anisotropic displacement parameter (isotropic for H) ratio for all t*

Atoms	β_{11} (*U*)	β_{22}	β_{33}	β_{12}	β_{13}	β_{23}
N1	0.0213 (11)	0.0016 (1)	0.0279 (13)	0.0032 (6)	0.0082 (9)	0.0027 (6)
N2	0.0270 (23)	0.0020 (1)	0.0145 (24)	−0.0007 (5)	0.0139 (18)	0.0006 (5)
N3	0.0268 (16)	0.0020 (1)	0.0192 (13)	0.0017 (6)	0.0055 (11)	0.0013 (6)
N4	0.0193 (22)	0.0015 (1)	0.0259 (24)	0.0002 (4)	−0.0034 (18)	0.0008 (4)
C1	0.0381 (32)	0.0017 (2)	0.0174 (29)	−0.0002 (6)	0.0040 (23)	−0.0013 (6)
C2	0.0170 (24)	0.0012 (2)	0.0406 (35)	−0.0014 (5)	0.0114 (24)	−0.0003 (6)
C3	0.0247 (15)	0.0020 (1)	0.0249 (14)	0.0010 (8)	−0.0036 (11)	−0.0011 (8)
C4	0.0225 (12)	0.0020 (1)	0.0192 (23)	0.0006 (7)	0.0035 (14)	0.0030 (8)
C5	0.0320 (36)	0.0023 (2)	0.0148 (26)	0.0011 (7)	0.0100 (24)	−0.0012 (6)
C6	0.0227 (30)	0.0014 (2)	0.0374 (37)	0.0000 (6)	0.0051 (26)	0.0027 (6)
O11	0.0353 (27)	0.0024 (2)	0.0314 (29)	0.0005 (5)	0.0074 (21)	−0.0016 (5)
O21	0.0372 (25)	0.0029 (2)	0.0474 (31)	−0.0019 (5)	0.0075 (21)	−0.0003 (6)
O31	0.0305 (26)	0.0013 (2)	0.0471 (31)	−0.0007 (4)	−0.0061 (19)	−0.0023 (5)
O41	0.0341 (35)	0.0018 (1)	0.0441 (28)	−0.0003 (5)	0.0034 (22)	−0.0006 (5)
C11	0.0361 (33)	0.0013 (2)	0.0493 (38)	−0.0004 (6)	0.0116 (28)	−0.0024 (6)
C21	0.0517 (43)	0.0018 (2)	0.0631 (48)	−0.0013 (7)	−0.0105 (36)	0.0006 (7)
C31	0.0504 (40)	0.0013 (2)	0.0366 (39)	−0.0032 (6)	−0.0047 (30)	−0.0025 (6)
C41	0.0547 (44)	0.0019 (2)	0.0335 (32)	−0.0018 (7)	−0.0173 (28)	−0.0004 (6)
C51	0.0452 (45)	0.0018 (2)	0.0645 (50)	0.0009 (8)	0.0165 (36)	−0.0008 (8)
C61	0.0338 (35)	0.0025 (2)	0.0325 (34)	0.0006 (7)	−0.0069 (27)	0.0008 (6)
C71	0.0279 (33)	0.0015 (2)	0.0326 (32)	0.0004 (6)	0.0085 (26)	−0.0009 (6)
C81	0.0312 (32)	0.0017 (2)	0.0222 (29)	−0.0014 (6)	−0.0086 (24)	0.0026 (6)
H2	0.46 (8)					
H31	0.50					

for example in $(C_{10}H_{21}NH_3)_2CdCl_4$ (Schenk & Chapuis, 1988). The packing of the suberic acid and hexamine will be discussed in §4.1.2 and §4.1.4.

For the hexamine, the amplitudes of the components of the atomic MF's along **b** extend up to 1 Å (Fig. 7). Along **a** and **c** the modulation amplitudes are much smaller. The modulation of the hexamine moiety is therefore transverse. The amplitudes of the atomic MF's for the suberic acid are comparable in three directions. The modulations have both transverse and longitudinal

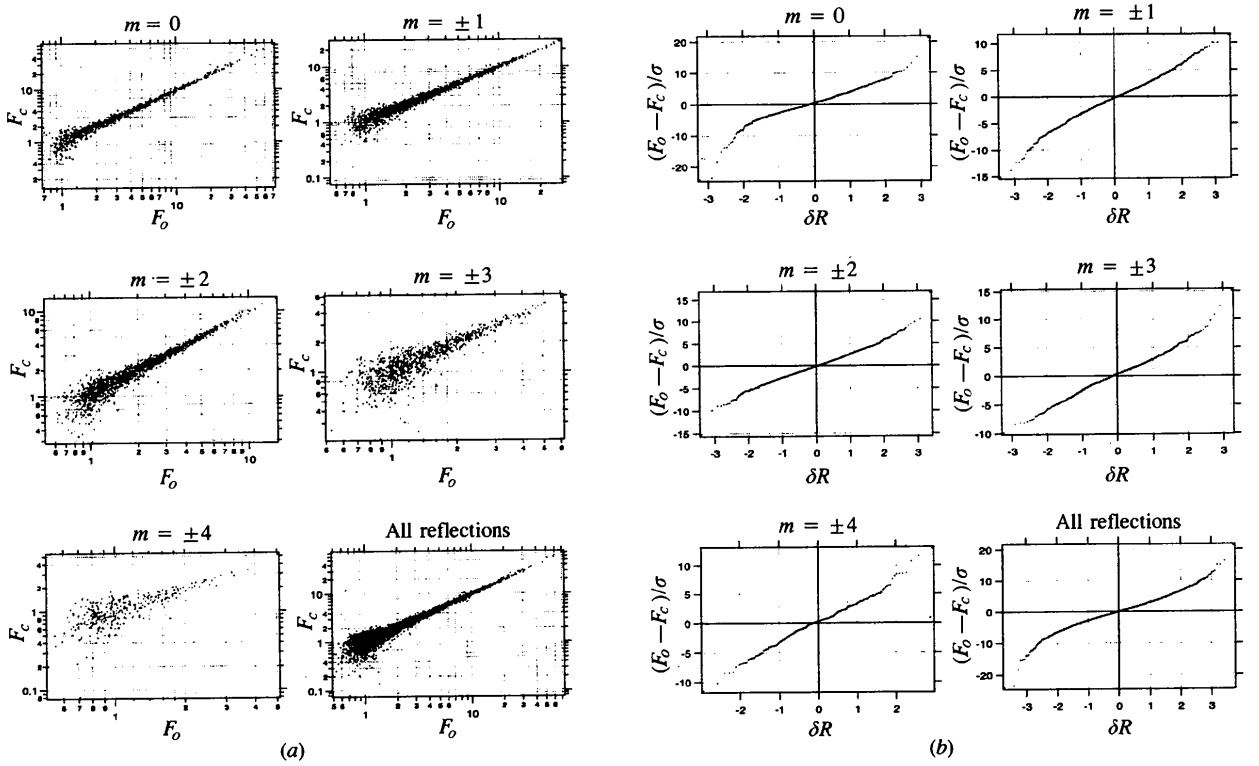

Fig. 5. (*a*) F_{calc} *versus* F_{obs}; (*b*) normal probability plots represented for different classes of reflections.

contributions. The MF amplitudes of the oxygens are especially strong and extend up to 1.5 Å (Fig. 7).

In order to emphasize the general behaviour of the strong modulation of the compound, a sequence of suberic acid chains and hexamines has been illustrated in Fig. 8 for 13 consecutive values of t.

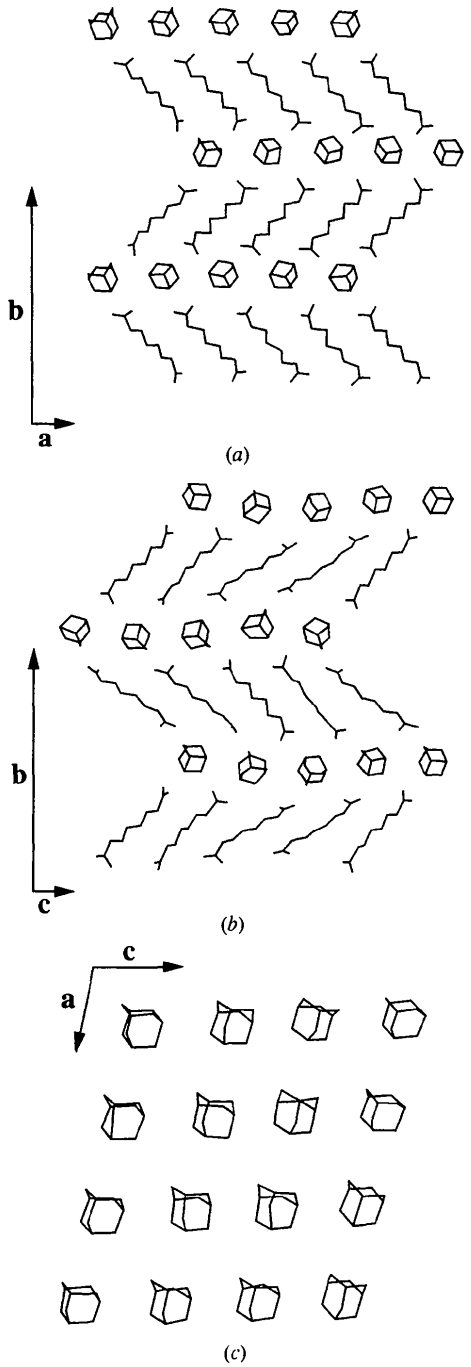

Fig. 6. (*a*) and (*b*) two projections of the incommensurate structure at t = 0.3. H atoms have been omitted for clarity. (*c*) Layer of hexamine units for the same value of t.

4.1.2. *The suberic acid chains.* A sheet of suberic acid chains is subdivided into two types of area. In each area, the zigzag planes and the chain axes are roughly parallel and the chains adopt a $T_{\parallel}$ packing according to the notation of Segerman (1965) and Abrahamsson, Dahlén, Löfgren & Pascher (1978). In an adjacent area the zigzag planes subtend an angle of $\sim 60°$ (Fig. 9) and the chain axes are not parallel, but form an angle that fluctuates with t. At the interfaces boundary effects are observed and neighbouring chains adopt intermediate directions.

The relative rotation of the chains reveals that they adopt essentially two orientations as a function of t (Fig. 10). The terminal COOH planes rotate in phase with the zigzag plane of the chains, although the amplitudes of rotation are different.

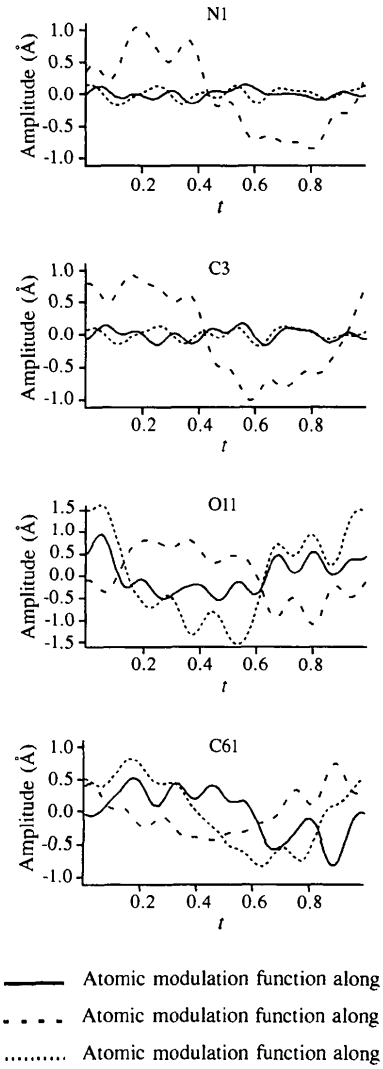

Fig. 7. Atomic MF's for some representative atoms of the hexamine suberate structure. Two atoms of the hexamine and two atoms of the suberic acid have been selected.

4.1.3. *The COOH groups.* Each layer of the suberic acid chains is linked to two layers of hexamine *via* hydrogen bonds between the proton of the COOH groups and the nitrogen of the hexamine. These hydrogen bonds are different at the two opposite suberic acid–hexamine interfaces (Figs. 11 and 12). It is also noteworthy that the two COOH groups of the suberic acid are not related by any symmetry operation.

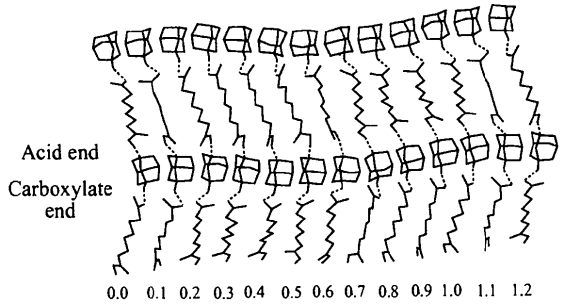

Fig. 8. Representation of a sequence of hexamine suberate molecules for different values of t with steps $\Delta t = 1/10$. The acid end, respectively, the carboxylate end, refers to the two independent COOH groups of a single chain. The hydrogen bonds are represented by dotted lines. The hydrogens of the methylene groups have been omitted. An arbitrary direction of the representation has been chosen to emphasize the modulation of the acid chain.

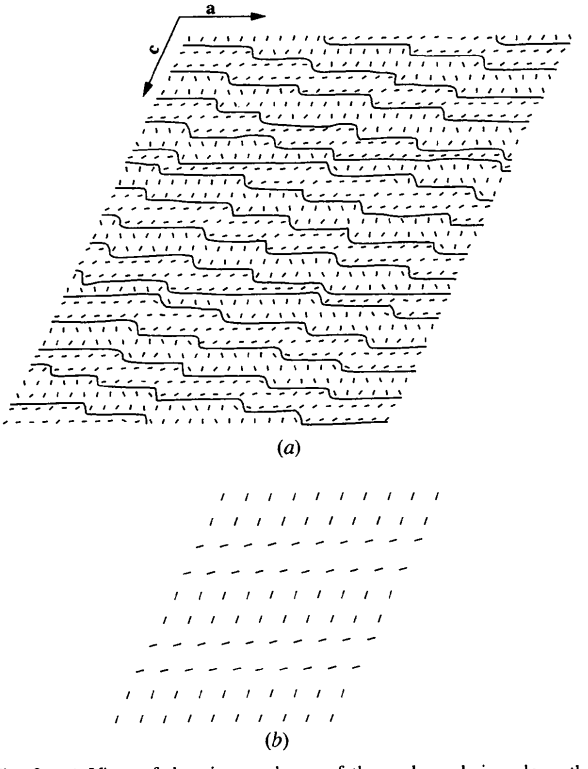

Fig. 9. (*a*) View of the zigzag planes of the carbon chains along the chain axes for the incommensurate crystal in $t = 0.0$ and (*b*) for the commensurate approximation.

For the H2—O11—C11—O21 group, the C11—O11 and C11—O21 distances are the same within standard errors (Fig. 11*a*). This group must therefore be considered as a carboxylate. The room-temperature data do not provide information on the precise nature of the hydrogen bonds, but the proton is probably located within the triangle O11···N2···O21 and participates in some rarer form of hydrogen bonds (*e.g.* three-centre bonds or bifurcated bonds). The different O···N2 distances (Fig. 12*a*) may be explained by the chain packing that forces the carboxylate group to change orientation as a function of t.

For the H31—O31—C81—O41 carboxyl group (Fig. 11*b*) at the other end of the chain, H31 is linked to O31 independently of t. The N4^{i}—O31 (see Table 6) distance varies between 2.6 and 2.8 Å, a typical N—O distance in the presence of a hydrogen bond. The second

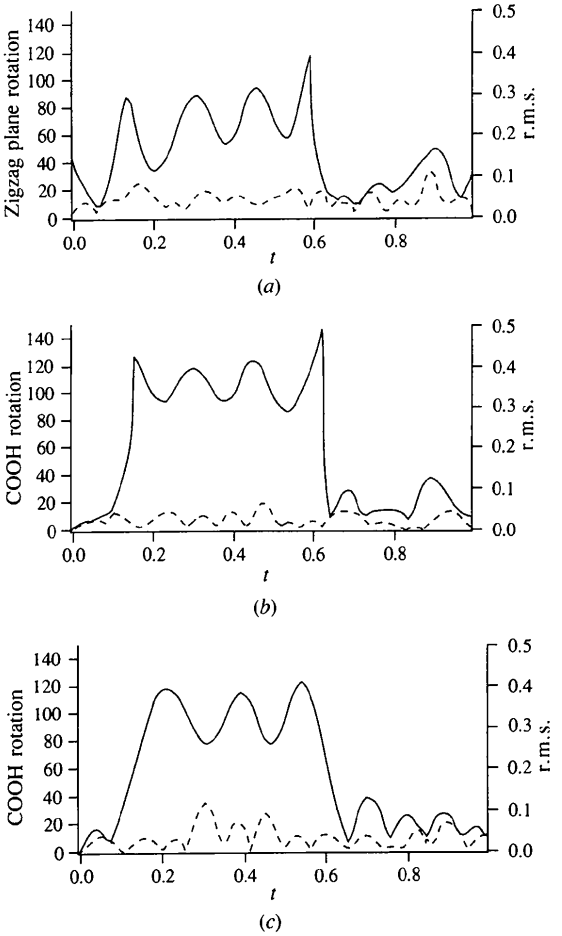

Fig. 10. (*a*) Angles between the zigzag plane (C11–C81) of a reference chain ($t = 0.0$) and the zigzag planes of 100 sequential values of t between 0 and 1. (*b*) Angles between the COO planes (O11—O21—C11—C21). (*c*) Angles between the COO planes (O31—O41—C81—C71). The dotted curves are the r.m.s. of the sum of the square distances between the atoms included in the plane and the average plane.

Table 6. *Selected bond distances (Å) and angles (°)*

The minimum, maximum and r.m.s. (with standard deviation) distances and angles are given. Δd is the interval between minimum and maximum values.

	Min.	Max.	$\bar{d}$ (°)	Δd (Δ°)
O11—C11	1.125	1.398	1.269 (55)	0.273
O21—C11	1.177	1.376	1.280 (51)	0.199
O31—C81	1.241	1.430	1.347 (46)	0.189
O41—C81	1.028	1.271	1.158 (54)	0.243
N4^{i}—H31	1.70	2.00	1.82 (15)	0.30
N2—H2	1.00	2.35	1.42 (16)	1.35
H2—O11	1.68	3.30	2.34 (16)	1.62
H2—O21	1.33	2.97	2.21 (17)	1.64
H31—O31	0.94	1.02	0.98 (15)	0.08
N2—O11	2.59	3.47	3.03 (5)	0.88
N4^{i}—O31	2.64	2.88	2.72 (5)	0.24
N2—O21	2.41	3.51	2.98 (5)	1.10
N4^{i}—O41	3.12	3.74	3.47 (5)	0.62
O11—C11—O21	106.56	133.19	119.98 (7)	26.63
O31—C81—O41	111.14	141.43	123.79 (6)	30.29
O11—C11—C21	98.61	133.47	117.62 (6)	34.86
O21—C11—C21	103.47	146.15	121.66 (7)	42.68
O31—C81—C71	87.66	126.29	109.75 (6)	38.63
O41—C81—C71	116.94	133.48	124.80 (6)	16.54
H2—N2—C1	63.47	166.83	104.54 (13)	103.36
H2—N2—C4	60.16	154.78	106.38 (12)	94.62
H2—N2—C6	55.19	160.58	115.20 (15)	105.39
H31—O31—C81	88.38	131.16	108.99 (19)	42.78
N2—H2—O11	69.83	165.49	110.84 (18)	95.66
N2—H2—O21	59.62	170.27	117.30 (19)	110.65
N4^{i}—H31—O31	133.00	171.10	152.10 (26)	38.10
H31—O31—C81—O41	0.16	359.99	186.63 (22)	359.83
O21—O11—C11—C21	157.09	195.51	178.21 (12)	38.42
O41—O31—C81—C71	156.65	213.31	183.10 (11)	56.66

Symmetry code: (i) $-x, y-\frac{1}{2}, -z-1, -t$.

oxygen O41 rotates around the N4^{i}—O31 axis and does not participate in the hydrogen bond (Fig. 12*b*).

One of the driving forces of the modulation is probably related to the ends of the chains.

4.1.4. *The hexamines.* In the hexamine sheets each molecule is surrounded by four others at the distance $\frac{1}{2}|(\mathbf{a}+\mathbf{c})|$ and two additional ones at |**a**|. This neighbourhood can be interpreted as a deformation of the closed-packed layer observed for the hexamine (Becka & Cruickshank, 1963) in the (110) plane (Fig. 13). The geometry of the hexamine molecule does not change significantly as a function of t and should be considered as a rigid body in future refinements.

4.2. *Justification of the selected model*

The reflection conditions derived from precession photographs indicate the superspace group $P2_1/m(\alpha 0\gamma)0s$. However, models refined in this superspace group did not yield satisfactory results. Therefore, the non-centrosymmetric superspace subgroup $P2_1(\alpha 0\gamma)$, which is also compatible with the systematic absences observed on precession

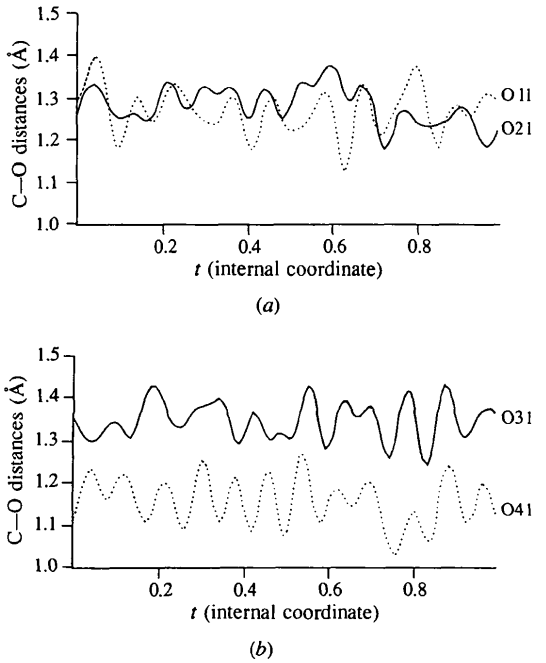

Fig. 11. (*a*) and (*b*) the C—O distances of the two COOH functional groups are represented for 100 values of t between 0.0 and 1.0.

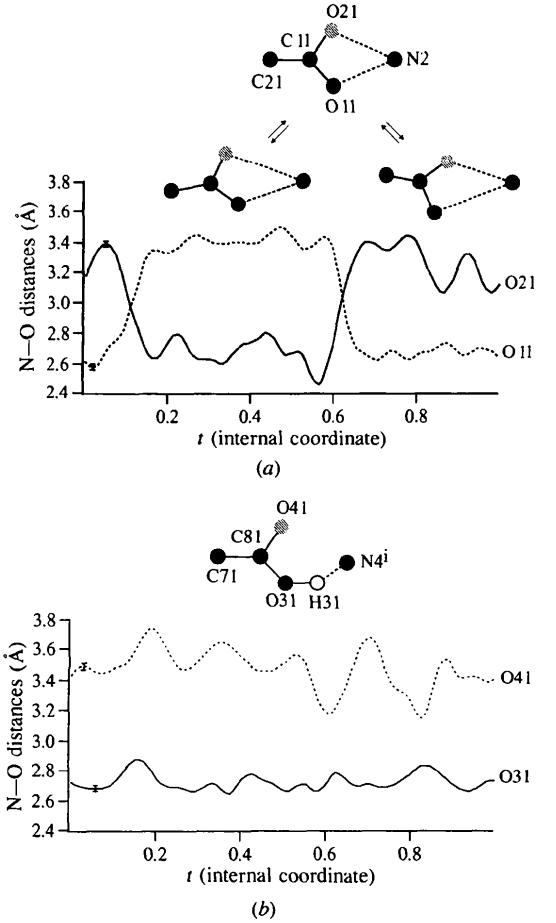

Fig. 12. (*a*) and (*b*) the N—O distances of the two COOH functional groups are represented for 100 values of t between 0.0 and 1.0.

photographs, was preferred. In this superspace group it was possible to refine a model consisting of one molecule of hexamine and one suberic acid chain (see §3.2). The fact that ($h0lm$, $m = 2n + 1$) structure factors calculated for this model were smaller than the average structure factor of the fourth-order satellites also justifies the choice of the superspace group. The main difference between both superspace groups concerns the COOH ends, which are independent in $P2_1(\alpha 0\gamma)$ (§4.1.3).

A model consisting of a superposition of the suberic acid molecules 1 and 4 observed in the commensurate approximation (Fig. 2) was also considered. In $P2_1(\alpha 0\gamma)$, atomic displacive modulations including up to fourth-order harmonics were refined for all atoms and an occupational modulation was applied to both chains. Even if the residual factors R were comparable to our selected model, the geometry of the chains was unsatisfactory, especially for one of them. Some atoms were not properly defined. Moreover, the difference-Fourier map based on the non-centrosymmetric model did not show any evidence for the presence of an additional chain.

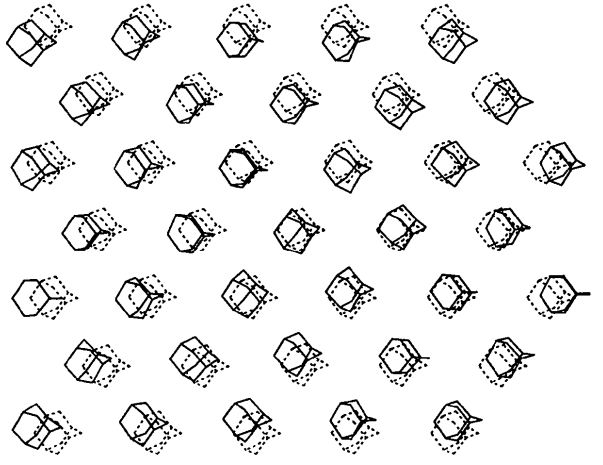

Fig. 13. Packing of the molecules of hexamine in the pure compound (dotted molecules) and in the incommensurate structure.

4.2.1. *Relation between harmonics and satellites orders.* This problem has been studied by Böhm (1975) and Korekawa (1967), even before superspace groups and MF's were invented. These studies revealed that the rule claiming that the satellites of a given order are caused by harmonics of the same order is only valid in the very special case of a purely occupational modulation. One may attempt to justify this rule for displacive modulations assuming that the amplitudes are small. By expanding the Bessel functions into series and retaining only the first term, one can obtain an expression for the structure-factor formula similar to the case of occupational modulation (Paciorek & Kucharczyk, 1985). This approximation is, however, so crude that it has never been used in practice.

In all other cases, especially for displacive modulations with arbitrary amplitudes, this rule is not valid. On the one hand, displacive modulations with one harmonic lead to diffraction patterns with satellites of all orders. On the other hand, an anharmonic displacive modulation (*e.g.* rectangular) can even give pseudo-extinction rules on satellites. In Böhm's seldom cited paper (Böhm, 1975) one may even find pictures as well as models with an infinite number of harmonics.

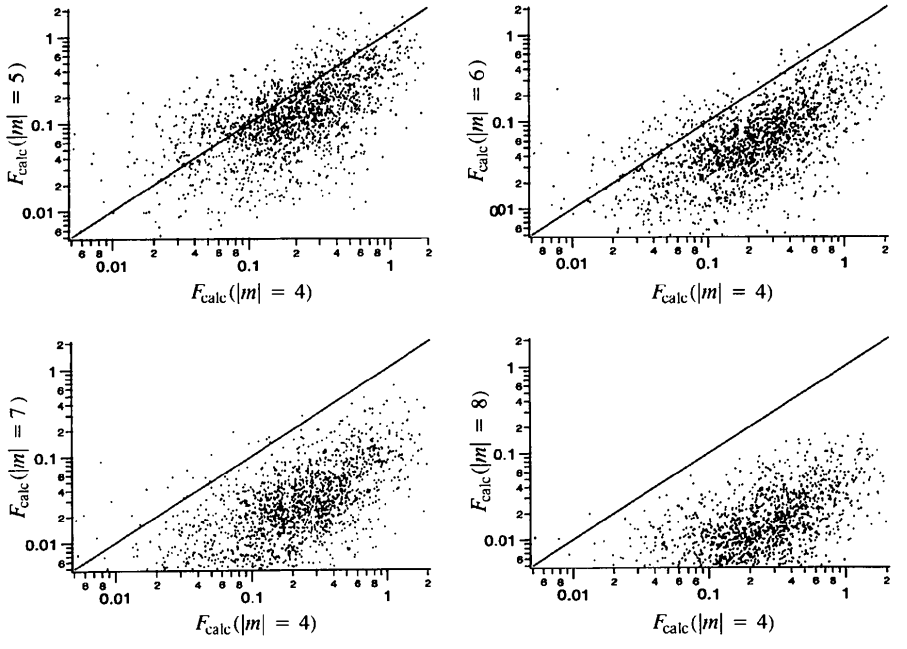

Fig. 14. F_{calc} of satellites ($hklm$), $|m| = 5$ to $|m| = 8$ *versus* F_{calc} of satellites ($hklm$), $|m| = 4$.

Of course, all such infinite Fourier series converge rapidly, but it is usually impossible to obtain reasonable approximations if only the first few terms are used. It is also generally untrue that adding more harmonics will perturb the shape of the MF's and in many cases it is just the opposite. It is even desirable to add more harmonics, because they have a smoothing effect on unwanted ripples and other oscillations. This effect is equivalent to the premature truncation of the Fourier series. The result of this extension may be better visible on some other quantites (*e.g.* interatomic distances) rather than directly on individual functions.

In the refinement of incommensurate structures the only limitation for the harmonic range is the reasonable ratio between the number of parameters and the number of observations. The significance of the parameters refined in the fit can be studied using standard tests (*e.g.* Hamilton test), as in a conventional structure refinement.

In order to verify that our model using eighth-order harmonics is not contradictory with the absence of measured satellites of order higher than four, the structure factors of satellites from order five to eight have been calculated and compared with the nearest satellites of order four (*e.g.*, for the reflection *hkl*4, the satellites with indices *hkl*5 to *hkl*8 have been calculated). The results are plotted in Fig. 14. One can observe that higher-order satellites are much weaker than the satellites of order four. Thus, our model based on harmonic terms up to eighth order does not contradict the experimental evidence that fourth-order satellites are at the limit of observability.

4.2.2. *The Axe correction.* The question must be raised why the maximum range of observed satellites is usually so small. A possible answer is the influence of thermal vibrations, especially the phason correction. The simple correction proposed by Axe is probably the right choice, at least as a first approximation. The influence of this correction has been reported several times (Axe, 1980). Omitting the Axe correction usually leads to an overall scaling ratio systematically greater than one for all satellites of order greater than one. This is especially true if the satellites are significantly weaker than the main reflections, as the scaling ratio is essentially determined by the main and first-order satellites. If higher-order satellites are strong, the least-squares refinement will terminate prematurely. Neglecting the Axe correction will affect the fit of practically all reflections. Introducing this correction will improve all of them. It is hard to find another single parameter causing such a large effect in the refinement (see Table 3).

5. Conclusions

The refinement of hexamine suberate has been a challenging task considering the large modulation amplitudes of the suberic acid molecule. Indeed, atomic displacive MF's cannot simulate such a molecular rotation without including a large number of harmonic terms (up to eighth order in the present report). In a previous paper (Paciorek, Bussien Gaillard, Schenk & Chapuis, 1996) it was shown, for a two-dimensional case, that the simplest harmonic modulation applied to the rotation angle of a molecule leads to an infinite Fourier series expansion for each displacive MF of the atoms belonging to the molecule. The same holds true for a modulation of the Euler angles in the three-dimensional case. Since the MSR program is limited to atomic MF's expressed as Fourier series, it requires the use of rather long expansions to reproduce rotations with large amplitudes. This approach is not exact and the number of parameters becomes easily excessive. We conclude that significant improvements are necessary to deal with similar incommensurate structures. The exact solution of rotational modulations is currently under development.

Even if the ADP's were not modulated as a function of t in the present refinement (in order to avoid an increase of the number of parameters), the orientation of the principal axes of the individual displacement ellipsoids should nevertheless be fitted to the orientations of the molecules for each value of t. So the question must be raised: what is the best way to vary the orientation of the displacement ellipsoids as a function of t without generating a large number of supplementary parameters to refine?

The structure revealed by the incommensurate refinement shows that each layer of suberic acid molecules is subdivided into two distinct areas (Fig. 9*a*), each of which is characterized by a dominant chain orientation. At the interfaces, boundary effects are observed and neighbouring chains adopt directions intermediate to the two limiting orientations. The commensurate approximation clearly loses this important feature (Fig. 9*b*). Theoretical studies on the packing of aliphatic chains (Abrahamsson, Dahlén, Löfgren & Pascher, 1978) do not list this packing mode, which is certainly not an energetically favourable case. The structure of suberic acid, for example (Housty & Hospital, 1965), contains only parallel chains.

The lattice periodicities of the hexamine in the incommensurate compound correspond very closely to the (110) planes of the cubic hexamine structure (Fig. 13). This very stable packing fixes the a, c and β cell parameters of the incommensurate structure. The origin of the double chain orientation must thus be found in the constraints imposed on the structure by the hexamine layer. Obviously, this constraint is too restrictive for the packing of the chains. Molecular modelling simulations do reveal that if the chains are constrained in a rigid framework of hexamine layers, an equilibrium consisting of two different chain orientations appears. This hypothesis on the origin of the modulation is further corroborated by the absence of incommensurability in other compounds containing suberic acid, but no hexamine (Vanier, Belanger-Gariepy

& Brisse, 1983). It is also noteworthy that the acid chains in these compounds do contain an inversion centre, whereas in the title compound the two terminal COOH groups of the suberic acid adopt independent and different geometries as a function of the internal coordinate t and thus remove the centre of inversion.

In the family of hexamine and diacids, two additional structures have been studied, namely the complexes formed by hexamine with azelaic (nine C atoms) and sebacic (ten C atoms) acids. A characteristic even–odd effect has been detected as in many other structures with chain packings. Crystals of the azelaic complex appear to be commensurate. Precession photographs revealed superstructure reflections below 263 K. The sebacic complex is also incommensurate and satellites up to sixth order have been detected. Preliminary refinements of this compound revealed a structure very similar to hexamine suberate.

The authors are greatly indebted to Bryan Craven and John Ruble for pointing out this interesting structure and for supplying the low-temperature lattice constants. The support of the Swiss National Science Foundation is gratefully acknowledged.

References

Abrahamsson, S., Dahlén, B., Löfgren, H. & Pascher, I. (1978). *Prog. Chem. Fats Other Lipids*, **16**, 125–143.

Axe, J. D. (1980). *Phys. Rev. B*, **21**, 4181–4190.

Becka, L. N. & Cruickshank, D. W. J. (1963). *Proc. R. Soc. London Ser. A*, **273**, 435–454.

Böhm, H. (1975). *Acta Cryst.* A**31**, 622–628.

Cummins, H. Z. (1990). *Phys. Rep.* **185**, 214–392.

Gao, Q., Weber, H. P. & Craven, B. (1994). *Acta Cryst.* B**50**, 695–703.

Housty, J. & Hospital, M. (1965). *Acta Cryst.* **18**, 753–755.

Johnson, C. K. (1965). *ORTEP*. Report ORNL-3974. Oak Ridge National Laboratory, Tennessee, USA.

Kobayashi, H. (1974). *Acta Cryst.* B**30**, 1010–1017.

Korekawa, M. (1967). *Theorie der Satellitenreflexe*. Habilitationsschrift der Ludwig-Maximilian-Universität München.

Paciorek, W. A. (1991). *Methods of Structural Analysis of Modulated Structures and Quasicrysals*, edited by J. M. Perez-Mato, F. J. Zúñiga & G. Madariaga, pp. 268–279. Singapore: World Scientific Publishing.

Paciorek, W. A. & Kucharczyk, D. (1985). *Acta Cryst.* A**41**, 462–466.

Paciorek, W. A., Bussien Gaillard, V., Schenk, K. & Chapuis, G. (1996). *Acta Cryst.* A**52**, 349–364.

Paciorek, W. A., Madariaga, G. & Zúñiga, F. J. (1991). *J. Appl. Cryst.* **24**, 66–70.

Rollet, J. S. (1965). In *Computing Methods in Crystallography*. Oxford: Pergamon Press.

Schenk, K. J & Chapuis, G. (1988). *J. Phys. Chem.* **92**, 7141–7147.

Segerman, E. (1965). *Acta Cryst.* **19**, 789–796.

Sheldrick, G. M. (1978). *SHELXTL. An Integrated System for Solving, Refining and Displaying Crystal Structures from Diffraction Data*. University of Göttingen, Germany.

Sheldrick, G. M. (1993). *SHELXL*93. University of Göttingen, Germany.

Smaalen, S. van (1995). *Cryst. Rev.* **4**, 79–202.

Vanier, M., Belanger-Gariepy, F. & Brisse, F. (1983). *Acta Cryst.* C**39**, 916–917.

Wolff, P. M. de, Janssen, T. & Janner, A. (1981). *Acta Cryst.* A**37**, 625–636.